33rd EPS Conference on Plasma Phys. Rome, 19 - 23 June 2006 ECA Vol.**30I**, P-1.197 (2006)

Blob dynamics in a hot plasma

J. Madsen[1], J. Staerk[1], V. Naulin[1], J. Juul Rasmussen[1],
A. Kendl[2], O.E. Garcia[1], and A. H. Nielsen[1]

[1] *Association EURATOM-Risoe National Laboratory, OPL-128, DK-4000 Roskilde Denmark*

[2] *Association EURATOM-ÖAW, Institute for Theoretical Physics, Leopold-Franzens University of Innsbruck, A-6020 Innsbruck, Austria.*

Experimental observations have revealed that the transport in the edge and scrape-off-layer (SOL) of toroidally magnetized plasmas is strongly intermittent and involves large outbreaks of hot plasma. These structures, often referred to as "blobs", are formed near the last closed flux surface (LCFS) and propagate far into the SOL, see e.g., [1] for references. They have a profound influence on the pressure profiles in the SOL, the ensuing parallel flows, and the power deposition on plasma facing components. The basic blob dynamics is well described in terms of nonlinear interchange motions in the limit of cold ions [1, 2]. Experimental observations, however, show that the ion temperature in the blobs may exceed the electron temperature due to the rapid loss of hot electrons to the divertor target plates.

We present the first investigations of the influence of finite ion temperature and finite Lamor radius (FLR) effects on the propagation of isolated blob structures by applying a gyro-fluid model. The blob propagation properties are investigated for a wide range of ion to electron temperature ratios and are found to be significantly altered by large ion temperatures. Finite ion temperature effects prevent nonlinear fragmentation and thus enhance the radial advection properties of such filamentary structures, which may result in hazardous power deposition on the main chamber walls.

We have derived a set of nonlocal gyro-fluid equations for two-dimensional interchange dynamics at the outboard midplane of a toroidally magnetized plasma on the basis of the two-moment equations in Ref. [3]. These equations describe the evolution of the particle densities and temperatures in a slab plane (x corresponds to the radial and y to the poloidal direction) perpendicular to the confining magnetic field along the z-axis and contains the dynamical evolution of the profiles. Parallel sound wave dynamics and electromagnetic effects are neglected. We restrict our investigations to the case of constant ion and electron temperature. The equations for the ion, n_i, and electron, n_e, densities read:

$$\partial_t n_i + [\psi, n_i] = -n_i \mathscr{C}(\psi) - T_i \mathscr{C}(n_i) + \mu \nabla^2 n_i, \quad (1)$$

$$\partial_t n_e + [\phi, n_e] = -n_e \mathscr{C}(\phi) + \mathscr{C}(n_e) + \mu \nabla^2 n_e, \quad (2)$$

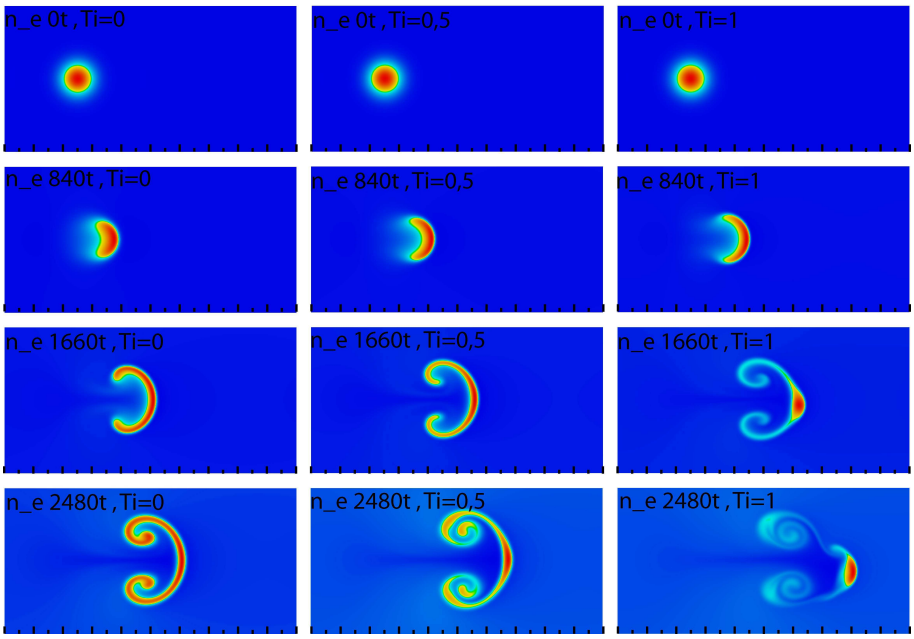

Figure 1: *Evolution of the electron density for an initial blob at* $\mathbf{x}_0 = (L/4, L/2)$. *Shown* $0 \leq x \leq L$ *and* $L/4 \leq y \leq 3L/4$.

where $[\phi, n] \equiv -\nabla\phi \times \hat{\mathbf{z}} \cdot \nabla n = \partial_x \phi \partial_y n - \partial_x n \partial_y \phi$ designates the advection with the $E \times B$-velocity. Due to their finite Lamor radii the ions feel a reduced convection velocity with the gyro-reduced potential ψ given by $\psi = \phi_G - v_E^2/2$ where $\phi_G = \Gamma_1 \phi$ is the gyro averaged potential and the last term represents the gyro screening effect, with $\mathbf{v}_E = -\nabla\phi \times \hat{\mathbf{z}}$. The FLR effect on the electrons is smaller by the mass radius and neglected. Equations (1) and (2) are coupled by the polarization equation with the assumption of quasi-neutrality (see e.g., [4]):

$$\Gamma_1 n_i + (1/T_i)(\Gamma_0 - 1)\phi = n_e. \tag{3}$$

The gyro-averaging operators are defined as: $\Gamma_0 = [1 - \rho_i^2 \nabla^2]^{-1}$ and $\Gamma_1 = [1 - (1/2)\rho_i^2 \nabla^2]^{-1}$ where $\rho_i = \sqrt{T_i/M}/\omega_{ci}$ is the ion Lamor radius and ω_{ci} is the gyro-frequency. The quantities are normalized as given in Ref. [1], i.e., time is normalized with ω_{ci}^{-1}, length with $\rho_s = c_s/\omega_{ci}$, where $c_s = \sqrt{T_e/M}$ and potential by T_e/e. The ion temperature T_i, which is a parameter in this formulation, is normalized with respect to the electron temperature T_e. The density is normalized by a uniform background density N. In Eqs. (1 - 2) $\mathscr{C}(\cdot) = -\xi \partial_y$ designates the curvature operator in the slab geometry, $\xi = \rho_s/R_0$, where R_0 is the major radius of the toroidal plasma. Finally, μ represents the collisional diffusion coefficient. For cold ions ($T_i = 0$) Eqs. (1 - 3) reduce to a system of 2D cold-ion fluid equations resembling the Risø ESEL-model for constant electron temperature [1].

For the purpose of investigating the propagation properties of isolated blob structures Eqs. (1

- 3) are solved numerically on a periodic domain by means of a de-aliased pseudo-spectral code. Typically we have used at least 1024×1024 modes on a square of length $L = 256$.

The blob structures are initialized with with a symmetric distribution of the densities: $n_e(\mathbf{x}, t = 0) = n_i(\mathbf{x}, t = 0) = 1 + \Delta n \exp\left[-(\mathbf{x} - \mathbf{x}_0)^2/2d^2\right]$. For the cases shown here we have used $\Delta n = 0.5$ and $d = 10$, but we have verified that the global propagation features do not depend dramatically on the specific parameters as long as $d^2 \gg 1$.

In Fig. 1 we show the evolution of the electron density (the ion density is evolving similarly) of the localized blob structure for different ion temperatures. Initially the ion and electron density perturbations are identically and the potential perturbation is vanishing in the limit of cold ions. This implies that there is no initial flow field, which, however, subsequently will build up from the polarization of the blob structure due to the curvature terms on the right hand side of Eqs. (1 - 2) and the densities will be advected radially outward (cf. [2]).

For finite ion temperatures the gyro averaging of the ion density, described by the first term on the left hand side of Eq. (3) results in an initial potential perturbation, which is small and the main source for the developing flow field is the polarization due to the curvature terms. For finite ion temperatures this polarization is enhanced as seen from the second term on the right side of Eq. (1). From the results in Fig. 1 we emphasize: For $T_i = 0$ the propagation resembles the evolution for the cold ion fluid model [2]. For finite ion temperature the blob acceleration increases, see also Fig. 2, due to the enhanced polarization effect described above. Additionally, we observe an increasing concentration of the density at the front of the structure, while the density in the trailing "arms" is less pronounced and decays more rapidly for increasing ion temperature. While the increased concentration of the density at the front can be ascribed partly due to the stronger acceleration and the FLR effects, the slight downward motion is also related to the curvature acting on the potentials (first terms on the right hand side of Eqs. (1 - 2)). To further quantify the motion of the blobs we plot the radial component of the center of mass velocity, V_{com} in Fig. 2, where

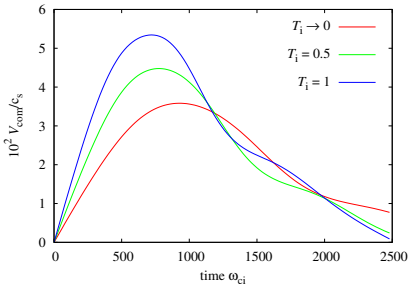

Figure 2: *Center of mass velocity.*

$$V_{com} = \frac{\int n_e v_x \, d\mathbf{x}}{\int n_e \, d\mathbf{x}}; \qquad v_x = -\partial_y \phi.$$

We observe an enhanced acceleration and find that the maximum velocity is increasing with T_i roughly proportional to $\sqrt{1 + T_i}$. This implies that the maximum velocity also for finite ion temperatures scales with the ion sound speed ($c_i = \sqrt{1 + T_i} c_s$) and the maximum blob velocity

for the present parameters is $\approx 0.035 c_i$). At late times the velocity decreases due to mixing and dissipative effects. A detailed investigation of the scaling of the velocity with blob parameters is presented in [2] for the cold ion, fluid model. A limited parameter scan for finite T_i indicates a similar dependence.

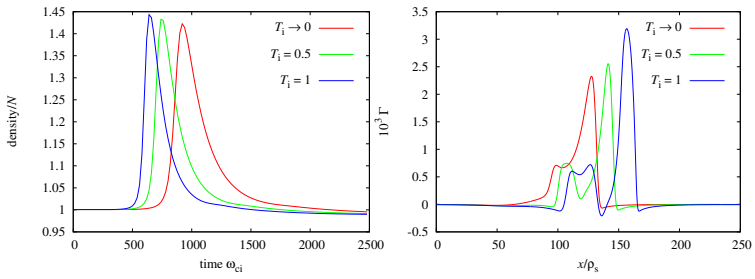

Figure 3: *Temporal evolution of density at* $x = 100$ *and at the y-position where amplitude is maximum (left panel). Flux at t = 1660 (right panel).*

In Fig. 3 we show the structure of the blobs as it would be recorded by a probe at a fixed position where the maximum of the blob passes. The typical behavior of a fast rising front followed by a slower decaying tail remains for finite ion temperatures. We observe further that the blob amplitude decays slower for increasing ion temperature. In the right panel of Fig. 3 we plot the convective flux ($\Gamma = (1/L)\int n_e v_x\, dy$) averaged over the y-direction. The flux is strongly localized and enhanced for finite ion temperatures.

Investigations of localized blob structures for a range of ion to electron temperature ratios show that the details of the propagation properties are significantly altered by finite ion temperature. The radial acceleration of the blobs is enhanced, but the scaling of the maximum blob velocity is still following the effective ion acoustic velocity. Nonlinear fragmentation of the blobs is prevented, leading to a more concentrated density structure, which will thus enhance the radial density flux associated with the blob filamentary structures. This may result in enhanced hazardous power deposition on plasma facing components. The inclusion of temperature variation in the model is in progress.

References

[1] O. E. Garcia, V. Naulin, A. H. Nielsen, and J. Juul Rasmussen, Phys. Rev. Lett. **92**, 165003 (2004); Phys. Plasmas **12**, 062309 (2005); Physica Scripta **T 122**, 89 (2006).

[2] O. E. Garcia, N. H. Bian, V. Naulin, A. H. Nielsen, and J. Juul Rasmussen, Phys. Plasmas **12**, 090701 (2005); O. E. Garcia, N. H. Bian, and W. Fundamenski, submitted for Phys. Plasmas (2006).

[3] D. Strintzi and B. D. Scott Phys. Plasmas **11**, 5452, (2004).

[4] B. D. Scott, Phys. Plasmas **12**, 102307 (2005).